Water-Soluble Fe(II) Complexes for Theranostic Application: Synthesis, Photoacoustic Imaging, and Photothermal Conversion

Maeva Delcroix, Anil Reddy Marri, Stéphane Parant, Philippe Gros, Mathilde Bouché

Water-soluble Fe(II) complexes for theranostic application: Synthesis, photoacoustic imaging and photothermal conversion

Maeva Delcroix,[a] Anil Reddy Marri,[a,b] Stéphane Parant,[a] Philippe C. Gros,[a] Mathilde Bouché[a,*]

[a] Maeva Delcroix, Dr. Anil Reddy Marri, Stéphane Parant, Dr. Philippe C. Gros, Dr. Mathilde Bouché
Université de Lorraine, CNRS, L2CM UMR 7053, F-54000 Nancy, France
[b] Dr. Anil Reddy Marri
Department of Chemistry, North Carolina State University, 851 Main Campus Drive, Raleigh (NC), 27695-8204, USA

Corresponding author: Mathilde Bouché, ORCID: 0000-0003-2707-1290
Mathilde.bouche@univ-lorraine.fr

Abstract:
Significant effort focused on developing photoactivatable theranostics for localized image guided therapy of cancer by thermal ablation. In this context iron complexes were recently identified as photoactivatable theranostic agents with adequate biocompatibility and body clearance. Herein, a series of Fe(II) complexes bearing polypyridine or N-heterocyclic carbenes is reported that rely on rational complex engineering to red-shift their MLCT based excited-state deactivation *via* a straightforward approach. The non-radiative decay of their MLCT upon irradiation is exploited for theranostic purpose by combining both tracking in photoacoustic imaging (PA) and photothermal therapy (PTT). The influence of structural modifications introduced herein on the complexes' solubility and stability in biorelevant aqueous media is discussed. The relationship between complexes' design, production of contrast in photoacoustic and photothermal efficiency are explored to develop tailored PA/PTT theranostic agents.

Introduction

Therapeutic agents that are trackable by medical imaging, commonly referred to as theranostics, are a promising class of drug candidates for the treatment of resistant cancers. It provides critical information on drug's real-time pharmacokinetics, particularly *in situ* tracking of the accumulation and elimination route. This theranostic approach notably highlighted the ability of some drug candidates to accumulate in tumors *in vivo*,[1] the *in vivo* stability of metal-ligand bond,[2] or the intracellular localization of the complexes.[3] A promising avenue for theranostic imaging is photoacoustic imaging (PA), a non-invasive imaging modality with hundred micrometers resolution, several centimeters imaging depth and low cost.[4] PA relies on the 'light-in sound-out principle', *i.e.* photoactivation of an agent capable to convert absorbed light into heat for thermal expansion of its surroundings and acoustic waves production. This ability of photothermal agents to convert light into heat is also exploited in photothermal therapy (PTT) for a cost-efficient and precise treatment of the diseased tissues.[5] The selectivity toward cancer cells provided by drug photoactivation is of foremost importance to limit off-target side effects and reduce drugs' therapeutic

dose.[6] Additionally, therapy *via* heat production can overcome cancer resistance by evading cells' reparation system, although a maximum temperature threshold of 43°C was fixed beyond which thermal damages increase together with temperature.[7] Typical PA and PTT setups favor near-infrared (NIR) light sources to limit thermal injuries by using less energetic wavelengths, and for reduced light attenuation by the tissues and endogenous molecules, particularly hemoglobin and deoxyhemoglobin.[8] As theranostics based on PA/PTT combination are receiving considerable interest, the development of water soluble theranostics that are accessible in a straightforward manner and can be easily finetuned to achieve NIR photoactivation is a hot topic.[9]

Theranostics are typically metal-based nanoparticles or organic semi-conducting particles that often involve systems with a complex design.[10] Therefore, finetuning their structure to achieve optimized optical and physico-chemical properties can be costly and demanding. On the other hand, polypyridine iron complexes are promising dual PA/PTT theranostic candidates owing to their intense absorption and straightforward structural modulation. The photophysics of octahedral Fe(II) complexes with a low spin $3d^6$ configuration are well-established,[11] such complexes typically displaying both highest occupied molecular orbital (HOMO) and lowest unoccupied molecular orbital (LUMO) that are metal-centered, *i.e.* t_2g and e_g* respectively. Hence, upon light absorption, since d-d transitions are forbidden, instead a metal-to-ligand charge transfer (MLCT) transition occurs in such complexes. It rapidly deactivates through low-lying metal centered states in a non-radiative manner and no competitive fluorescence or singlet oxygen production occurs. Recently, exploiting the MLCT transition of iron-bisterpyridine complexes proved of interest for PA.[12] While it highlighted the inherent benefits of this family for PA imaging, expanding the scope of such complexes is required to access adequate optical and physico-chemical properties for theranostic applications.

Herein, we propose a simple and straightforward route toward water-soluble and highly stable Fe(II) complexes. The rational design of Fe(II) complexes bearing moderate to strong field ligands, *i.e.* terpyridine (tpy) and 4-pyridin-2,6-bis N-heterocyclic carbene-pyridine (NHC), referred to as (C^N^C), is reported herein to access photostable complexes capable of light-triggered heat production due to a very short lived MLCT transition.[11] All the complexes proved efficient for contrast production in PA and photothermal conversion in PTT. Furthermore, a straightforward structural variation of the complexes by quaternization into pyridinium successfully prompted a red-shift of their MLCT, hence allowing enhanced PA and PTT efficiencies at irradiation wavelengths close to the near-infrared region (NIR). Finally, we highlight herein the potential for PA/PTT theranostics of the Fe(II)-(C^N^C) derivatives where the inert Fe-NHC interaction results in high stability of the complex towards both photobleaching and biological medium. Furthermore, this (C^N^C)-based complex is found to display a dramatic bathochromic shift of over 80 nm of its MLCT upon methylation, hence making them promising for further consideration as theranostics that might find application in the image guided therapy of resistant cancers.

Results and Discussion

Synthesis and Characterization

Pyridine-functionalized terpyridine ligands were selected owing to their protonatable nature that is anticipated to promote water-solubility, and considering their straightforward

synthesis by Krönke reaction ensuring isolation of the ligand in sizeable quantities. Pyridines possess high electron withdrawing character that is anticipated to affect the ligands' field, and exploring the influence of their orientation, *i.e.* ortho or meta or para oriented pyridines on the optical properties of the corresponding Fe(II) complexes is proposed. The three terpyridines **1a-c** were synthesized in high yields through a modified Krönke reaction proceeding at room temperature, hence limiting the formation of side-products and making it eventually more scalable.[13] Characterizations were in accordance with previous reports.[14] Further coordination to the iron chloride precursor in a 1:2 metal:ligand ratio according to reported procedure[15] and isolation by precipitation in diethyl ether afforded the corresponding homoleptic complexes **2a-c** as their water soluble chloride salts, chloride ion being non-toxic (Scheme 1). Successful coordination was confirmed by ^{1}H NMR with a significant downfield shift up to 9.5ppm of the singlet signal corresponding to the 3' and 5' protons of the tpy. Complexes' protonation to tetra-charged complexes **3a-c**, which is expected to boost their physico- and photo-activity, was achieved quantitatively using aqueous HCl. Furthermore, bis-methylation of complexes **2a-c** to the corresponding methyl-pyridinium complexes **4a-c** is anticipated to achieve enhanced electron withdrawing effect and stability, and proceeded at room temperature at a reaction rate controlled by nitrogen's electronic density, *i.e.* a decreased reaction rate was observed from **4c**>**4b**>**4a**. This is surprising as a moderate torsion angle between the pyridine and tpy ligand in the complex **2a** was observed in solid state by X-ray diffraction.[14a] Of note, a protocol of late-stage pyridine functionalization was preferred to the previously reported synthesis[16] as it offers greater versatility in view of further adapting this approach to the functionalization with expensive moieties such as fluorophores, vectors and so forth. A general downfield shift of the protons' signals was observed in ^{1}H NMR upon methylation to **4a-c**, which is coherent with the pyridinium's enhanced electron withdrawing character over non-quaternized pyridine.

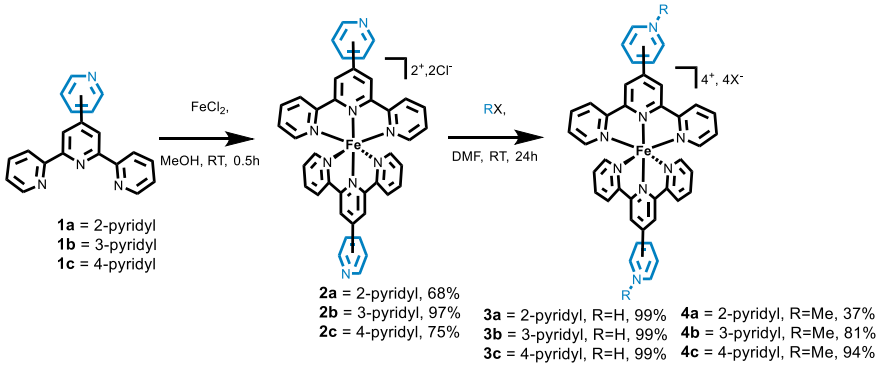

Scheme 1. Synthesis of the Fe(II)-terpyridine complexes studied in this work

As the metal-ligand bonds' stability in biological media is a key parameter for further development of theranostics, we propose herein an alternative to well-known tpy ligands with the use of pyridin-2,6-bis N-heterocyclic carbene-pyridine (C^N^C) ligands, that incorporate N-heterocyclic carbenes (NHCs) that are notorious for forming stable complexes (Scheme 2).[17] Hence, the ligand precursor **5** was obtained in 2 steps by Suzuki coupling of pyridin-4-yl boronic acid with 4-iodo-2,6-dichloropyridine, followed by reaction with methylimidazole through a different protocol than reported elsewhere.[11e] This imidazolium salt was further deprotonated and coordinated *in situ* to the iron precursor to yield the corresponding [Fe(C^N^C)$_2$]2Cl complex **6**. The complete disappearance of the

singlet corresponding to the NC*H*N proton in the ^{1}H NMR spectrum of **6** attests the successful imidazolium salts' deprotonation and carbenes' coordination to the metal. The desired quaternized complex **7** is obtained *via* a similar approach to its terpyridine counterparts **4a-c**, *i.e.* in the presence of iodomethane, and shows overall downfield shifted ^{1}H NMR signals compared to its non-methylated counterpart **6**.

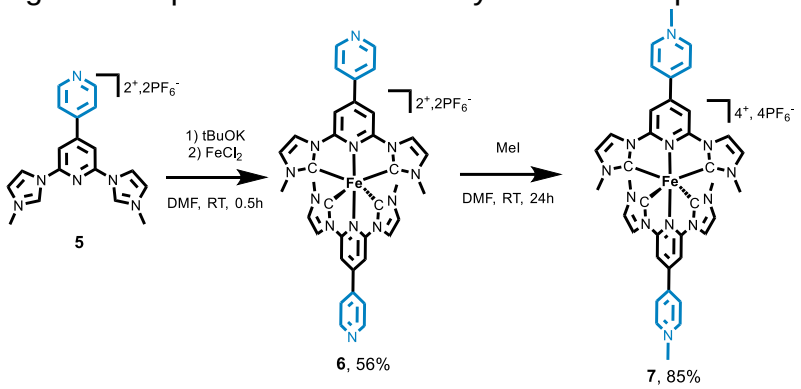

Scheme 2. Synthesis of the Fe(II)-NHC derivative **7**

Photophysical and physico-chemical properties in water and bio-relevant medium

The photophysical properties of all the complexes were investigated by absorbance spectroscopy (Table S1). As anticipated, the dicationic complexes **2a-c** showed an intense band around 575 nm, corresponding to a MLCT type transition, and the corresponding epsilon values in water are comparable to those reported in acetonitrile (Fig. 1A).[15a] The pyridyl substitution pattern, *i.e.* ortho, meta, para, has a negligible influence on the MLCT absorption shift of complexes **2a-c**. For complex **6**, two MLCT absorptions are observed with $\lambda_{N\text{-}Fe}$=510nm and $\lambda_{C\text{-}Fe}$=398nm (corresponding to the Fe-pyridine or Fe-NHC transitions respectively), which are significantly blue shifted compared to its terpyridine counterpart **2c** with $\lambda_{N\text{-}Fe}$=575 nm. This can be explained by the greater ligand field and σ-donation from the NHC to the metal compared to pyridines, and the larger bite-angle of the (C^N^C) ligand than terpyridine which allows enhanced orbital overlapping.[18] Protonation of the complex **2c** at pH3 is found to promote a significant bathochromic shift of the MLCT from $\lambda_{\mathbf{2c}}$=575nm to $\lambda_{\mathbf{3c}}$=590nm which is coherent with previous reports on comparable complexes,[19] while the other pyridinium complexes with different pyridine orientations show a negligible MLCT shift (Table S1). A comparable effect is observed upon protonation of complex **6** at pH 3.2 with a shift of 59 nm of the pyridine-Fe MLCT transition. A more pronounced effect on the absorbance $\lambda_{N\text{-}Fe}$ is observed upon methylation of both the terpyridine and the (C^N^C) complexes. Indeed, the MLCT absorption in **4c** was red-shifted by 22 nm up to 595nm. Furthermore, while the $\lambda_{N\text{-}Fe}$ in **6** is found at 510nm which is inadequate for biological use, its quaternization to **7** promotes a significant bathochromic shift up to 595nm. Such red-shift of 85nm is markedly greater than the 22 nm shift observed in complex **2c**, hence emphasizing the potential of the (C^N^C)-based family for further optimization of their optical properties towards the NIR. Overall, a red-shift of the MLCT absorption band is observed in the trend **2c**<**3c**<**4c** and **6**<**7** coherent with the increasing electron-withdrawing properties of the quaternized pyridine.

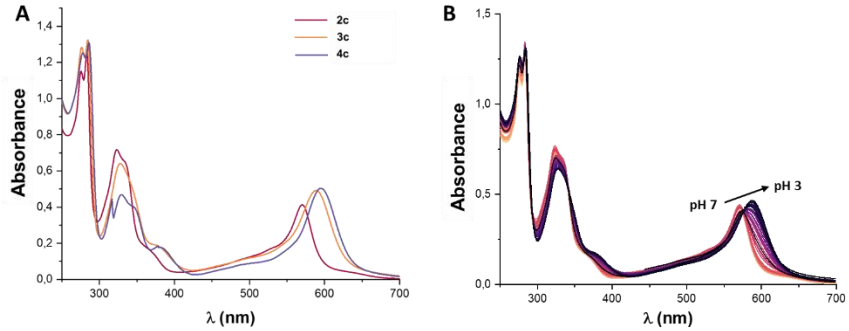

Fig. 1. A) Absorption spectra of the complexes **2c**, **3c** and **4c** in water (C=500 µM); B) speciation of **2c** as a function of the pH.

Water-solubility is a key parameter to consider in drug development as it contributes to dictating its absorption, distribution, metabolism, excretion, and toxicity (ADMET).[20] High water-solubility is desirable in order to limit drugs' off-target binding to the lipophilic pockets of important plasma proteins or metabolic enzymes. Log p values were measured by the 'shake flask' procedure as previously reported.[21] All the complexes **2a-c**, **4a-c** and **6**-**7** proved water-soluble showing negative log p values ranging from -1.8 to -3.6 (Table S2), hence suggesting their bioavailability. However, protonation of the pyridines in complexes **3a-c** was found to modulate the complexes' optical properties, notably by redshifting their absorption maxima, and must be considered owing to the pH variations existing in the body.[22] Hence, the pH dependent speciation was further explored for complexes **2c** and **3c** on the pH range 7 to 3. The spectrophotometric investigation of the species' existence as a function of pH depicted in Fig. 1B clearly showed the equilibrium between the protonated and non-protonated complexes **2c** and **3c** in the pH range of 3-5.8, beyond which no evolution is observed until pH 7. Of note, in this pH range, the MLCT absorption shows a decreased intensity, which can be ascribed to the coexistence of the protonated and non-protonated forms of the corresponding complex **2c**. This is coherent with the ligand's pKa that was predicted (by ACDLabs software) to be 4.2. A similar observation is made for complex **6** and its protonated counterpart, in the pH range 3.3-5.1, above which only complex **6** is observed (Fig. S1).

Stability in biological media is also a crucial parameter within the ADMET considerations, especially as it plays a role in maintaining the desired biological activity and hampering the formation of toxic metabolites that might result in significant deleterious effects. Gasser *et al.* emphasized the fact that rapid drug degradation in plasma is one of the exclusion criteria for drug development.[23] Therefore, the complexes **2a-c**, **4a-c** and **6**-**7** were incubated in serum over 72h and the complexes' stability was followed at selected time points (0, 12h, 48h, 72h) by UV-Visible absorption spectroscopy, monitoring an eventual decrease of the MLCT transition. No alteration of the MLCT transition intensity was observed irrespective of the ligands' nature or pyridine substitution, hence suggesting the stability of the metal-ligand bonds toward serum's proteins and the absence of ligand scrambling or transchelation events. Moreover, no blue shift was observed for **4a-c** and **6**-**7**, therefore suggesting the pyridinium stability under the tested conditions and methylation's irreversible character. Finally, the absorption spectra after 72h incubation proved unchanged from the corresponding complexes (Fig. S2), hence suggesting that

no non-covalent interaction occurred between the complexes and serum's proteins, which could eventually alter their biodistribution profile.[24]

Photoacoustic contrast production & photothermal efficiency

Thermal stability of the theranostic agent is of primary importance in view of theranostic use in PA or PTT, to maintain the trackability and therapeutic efficacy under repeated irradiation during a session and avoid the formation of toxic byproducts.[10] All the tested complexes proved stable toward repeated irradiation over 5 heating and cooling cycles, as confirmed by the retained photothermal efficiency, absorbance measurements (Fig. S3). Of note, the pyridiniums are found to be stable upon prolonged irradiation and do not undergo demethylation. Therefore, all the complexes tested herein showed adequate stability for use as photoactivated agent in PA or PTT. For the PA experiments presented herein, fresh solutions of the complexes in deionized water (C=200-1000 µM) were loaded into PTFE tubes (inner diameter 0.81mm, wall thickness 0.05 mm), immerged into water and irradiated at selected wavelengths with a gain of 30dB. A representative cross-section view of the seven tubes mounted on a spherical holder is shown for example in Fig. 2A, and highlights the enhanced PA contrast produced by the quaternized complexes **4a-c** and **7** at 660nm. PA amplitude of all complexes is found to be concentration dependent (Fig. S4.) and to vary significantly depending on the irradiation wavelength (Fig. 2B). Indeed, PA amplitudes obtained under 580nm irradiation shown in Fig.2C suggest a production of contrast in PA that is similar among all the complexes. An exception is the non-quaternized (C^N^C) complex **6** which PA amplitude is found by far lower to the other complexes investigated herein, which was anticipated as its MLCT is blue-shifted compared to others. Importantly, while the PA amplitude produced by **2c** suffers a dramatic decrease when irradiated with less energetic wavelengths, *i.e.* 660nm, in the case of complex **4c** that was designed to boost its photoactivity close to the NIR, high PA amplitude is observed under such conditions. This behavior is also noticeable in the case of **7** that shows significantly retained PA contrast in the NIR (Fig. S5). Hence, we proved herein that a simple structural modification of Fe(II) complexes allows boosting their photophysical properties to enable PA imaging in the NIR.

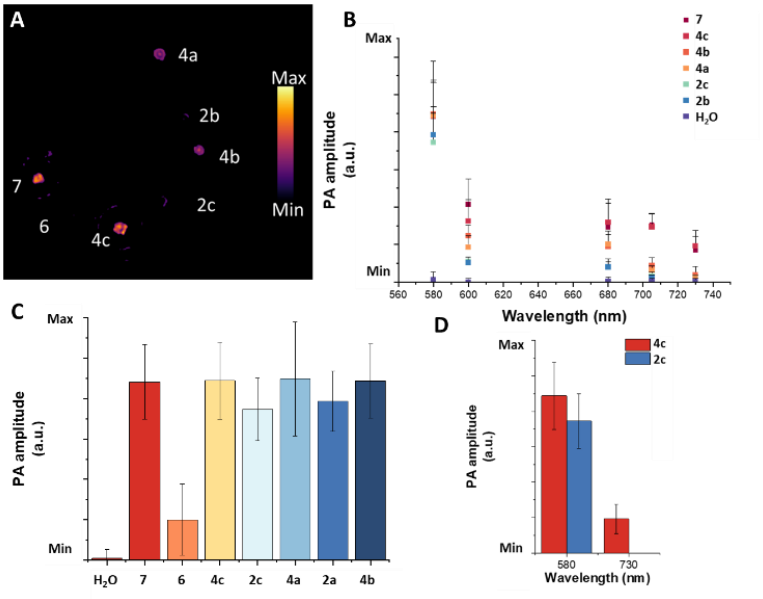

Fig. 2. Photoacoustic properties of the Fe(II) complexes (1mM in H_2O, 36°C). A) Representative PA cross-section view of the seven selected complexes (λ_{irrad}=660nm), B) variation of PA amplitude of the Fe(II) complexes depending on the irradiation wavelength, C) PA amplitude of selected complexes (λ_{irrad}=580nm), D) showing the greatest PA amplitude of quaternized complexes **7** and **4c** when irradiated with both visible and NIR wavelengths.

PTT investigation was performed on a custom setup using non-coherent light sources (LEDs) which are preferred to laser sources as it offers a cost-effective solution that is compatible with local treatment, although it imposes reduced light power and consequently limits the possible temperature raise.[25] Yet, it is worth mentioning that owing to the availability and ease of use of LEDs over lasers, a growing interest for LED-activated therapies has surged,[26] and a LEDs-based photoactivated therapy at 635nm was approved by FDA.[27] PTT acquisition are expressed as a function of the LEDs' irradiance, *i.e.* the light power received by a defined area corresponding to the samples' area, and since LEDs' power vary depending on the wavelength used, the irradiance vary accordingly.[24] On the other hand, the ΔT is linearly correlated to complexes' concentration (Fig. 3A). As anticipated based on PA observations, all the complexes produced a significant photothermal efficiency under 565nm irradiation for 5min, with an average ΔT~23°C for all the complexes tested (Fig. 3B). Such temperature increase is adequate for further PTT application in cancer therapy, as cancer cells are known to undergo apoptosis upon exposure to 43°C, *i.e.* upon a temperature increase of 7°C only.[7] Of note, overall greater ΔT are found at 660nm irradiation than 565nm due to the enhanced irradiance from the LED (0.3 $W.cm^{-2}$ and 0.6 $W.cm^{-2}$ respectively). Pleasantly, we observed that complexes **4c** and **7** successfully maintained a high light induced photothermal conversion upon irradiation with more redshifted LED sources, *i.e.* 660nm, while all the other complexes displayed reduced ΔT (Fig. 3C). The above-mentioned observation is in perfect agreement with the conclusions from PA imaging and confirm the rational design of complexes **4c** and **7** for boosting their potential in PA/PTT using NIR light irradiation.

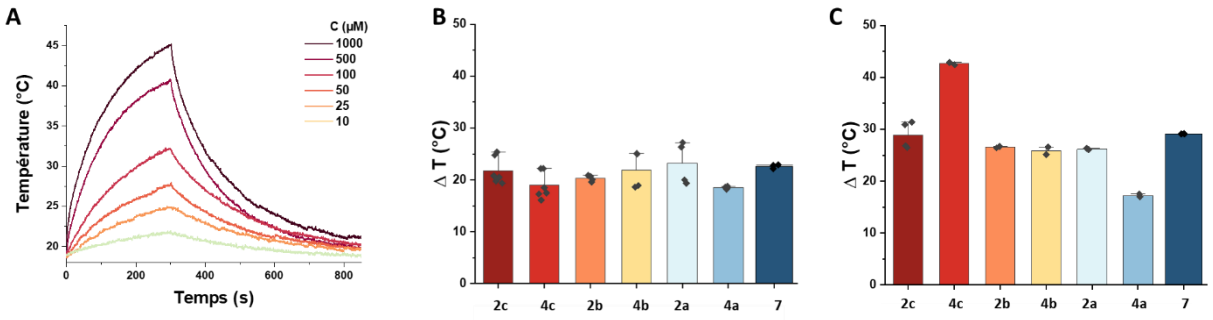

Fig. 3. Photothermal efficiency of the Fe(II) complexes (in H_2O, 5min irradiation). A) concentration dependent variation of ΔT for complex **2c** (565nm irradiation, range 1000-10µM), B) ΔT for complexes **2a-c** and **4a-c** under 565nm irradiation (1mM), C) ΔT for complexes **2a-c** and **4a-c** under 660nm irradiation (1mM).

Controlling the photoactivity of iron complexes is challenging and is a central question to multiple research fields aside biomedical applications.[11] Several strategies were proposed to exploit iron complexes' photosensitization of $^1O_2$ for PDT therapy, notably by conjugation to fluorophores active in the visible or NIR, which efficiently enabled photosensitization and DNA photocleavage properties.[28] Light activation of iron-based

chemotherapeutics has also been shown for small molecule release such as NO or CO release, in view of achieving a dual therapeutic activity.[29] On the other hand, non-radiative deactivation processes have rarely been explored in the design of iron-based chemotherapeutics.[27c] The ability of Fe(II)-bisterpyridine complexes for light photothermal conversion was highlighted by Tian *et al.* and further exploited for *in vivo* tracking of the complex's biodistribution with PAI, although the stability of [Fe(terpyridine)Cl_3] complex is compromised in biomimicking media.[12] However, we report herein a novel theranostic complex displaying enhanced photothermal stability and inertia that could be further used for PA/PTT theranostic applications.

Photoactivation in the NIR is highly desirable for deep light penetration and minimized light diffusion by the tissues, especially as major blood components, *i.e.* hemoglobin and deoxyhemoglobin, show decreased absorption beyond 600 nm and accordingly facilitated PA multiplexing. While the Fe(II)-NHC complex **7** successfully displayed a significantly redshifted MLCT absorption, expanding the scope of Fe(II) theranostic agents will be necessary to achieve NIR absorbing Fe(II)-NHC complexes. While the strong σ-donation and stability provided by the NHCs is beneficial in terms of stability, it also destabilizes the HOMO level hence inducing a bathochromic shift of the MLCT.[18] Gratefully, quaternization of the peripheral pyridine in **7** successfully redshifted the MLCT transition corresponding to N-Fe bond, which allowed photothermal activation under NIR irradiation. Yet, shifting the MLCT to the therapeutic window is currently ongoing to enhance the PAI/PTT activity of this family of complexes and make them more likely to clinical translation. Further development could include incorporation of a more electron-withdrawing moiety than pyridine in the structure[30] or enhancement of the π-conjugation in the ligand.[31] Indeed, a family of iron complexes that could be synthesized in a straightforward and cost-efficient manner and photoactivated in the NIR would be ideal for medical imaging guided precision medicine at low therapeutic dose.[27d] Finally, the quaternization approach used herein is currently being applied to complexes' functionalization with disease specific vectors to achieve a dual control over therapeutics' selectivity driven by vector-target affinity for dual selective photoactivatable theranostics.

Conclusion

We reported herein on the synthesis and photophysical characterization of a series of Fe(II) complexes bearing tridentate Schiff bases, namely terpyridines and bis-NHC ligands. We proposed a straightforward quaternization of the complexes to boost their solubility and photophysical properties, hence making them compatible for theranostic use under NIR irradiation. Exploiting their light triggered non-radiative deactivation pathway enabled their use as PA imaging agent observable under NIR irradiation. Promising PTT properties were also highlighted here using a LEDs-based setup, hence establishing those complexes as competent water-soluble theranostic agents that could be activated and tracked in the NIR. Overall, the design simplicity of the PA/PTT active complexes detailed herein highlight them as promising theranostics to further explore possibilities in optical imaging guided anticancer therapy.

Supporting Information

Additional references cited within the Supporting Information.[32]

Acknowledgements

The authors are grateful for financial support from the 'Agence Nationale de Recherche' (ANR-21-CE07-0023-01, to M.B.), from the European Regional Development Funds (Programme opérationnel FEDER-FSE Lorraine et Massif des Vosges 2014-2020/"Fire Light" project: "Photo-bio-active molecules and nanoparticles", from the CNRS and the University of Lorraine. The authors gratefully acknowledge the Platform PhotoNS of the L2CM Laboratory (University of Lorraine) and the mass spectrometry MassLor platform (University of Lorraine). ^{1}H and ^{13}C NMR spectra were recorded on a Bruker Avance III (400 MHz, 100.6 MHz respectively) on the CPM NMR facility (University of Lorraine). F. Dupire is acknowledged for performing mass spectrometry and P. Lemiere for purification with preparative HPLC. K. Selmeczi is acknowledged for valuable discussion.

Keywords: Bioinorganic chemistry; Iron; Optical properties; Photoacoustic imaging; Photothermal therapy.

Conflict of interest: The authors have no conflict of interest to declare.

Authors contribution: M.B. designed research. M.D., A.R.M., S.P., P.C.G. and M.B. conceived, designed and performed the chemical experiments. M.B. wrote the paper and M.D., A.R.M., S.P., and P.C.G. participated in manuscript writing.

Reference section:

1) R. Lescure, M. Privat, J. Pliquett, A. Massot, O. Baffroy, B. Busser, P.S. Bellaye, B. Collin, F. Denat, A. Bettaieb, L. Sancey, C. Paul, E. Bodio, *Eur. J. Med. Chem.* **2021**, *220*, 113483.

2a) B. Rousselle, A. Massot, M. Privat, L. Dondaine, A. Trommenschlager, F. Bouyer, J. Bayardon, F. Ghiringhelli, A. Bettaieb, C. Goze, C. Paul, R. Malacea-Kabbara, E. Bodio, *ChemMedChem*. **2022**, *17* (11), e202100773; b) H. Yao, G. Zhu, *Dalton Trans*. **2022**, *51*, 5394.

3a) F. Ai, T. Sun, Z. Xu, Z. Wang, W. Kong, W. To, F. Wang, G. Zhu, *Dalton Trans.* **2016**, *45*, 13052; b) N. Wang, Z. Deng, Q. Zhu, J. Zhao, K. Xie, P. Shi, Z. Wang, X. Chen, F. Wang, J. Shi, G. Zhu, *Chem. Sci.* **2021**, *12*, 14353; c) A. Trommenschlager, F. Chotard, B. Bertrand, S. Amor, P. Richard, A. Bettaïeb, C. Paul, J.-L. Connat, P. Le Gendre, E. Bodio, *ChemMedChem*. **2018**, *13* (22), 2408; d) Z. Liu, J. Li, D. Kong, M. Tian, Y. Zhao, Z. Xu, W. Gao, Y. Zhou, *Eur. J. Inorg. Chem.* **2019**, *2019* (2), 287, e) S. Harlepp, E. Chardon, M. Bouché, G. Dahm, M. Maaloun, S. Bellemin-Laponnaz, *Int. J. Mol. Sci.* **2019**, *20*, 4198.

4a) J. Zhou, J.V. Jokerst, *Photoacoustics* **2020**, *20*, 100211; b) E. Bossy, S. Gigan, *Photoacoustics* **2016**, *4* (1), 22.

5a) Y. Liu, P. Bhattarai, Z. Dai, X. Chen, *Chem. Soc. Rev.* **2019**, *48* (7), 2053; 5b) J. Sun, H. Zhao, W. Xu, G.-Q. Jiang, *Front. Chem.* **2022**, *10*, 1024177; 5c) H.S. Han, K.Y. Choi, *Biomedicines* **2021**, *9* (3), 305; 5d) B.-D. Zheng, Q.-X. He, X. Li, J. Yoon, J.-D. Huang, *Coord. Chem. Rev.* **2021**, *426*, 213548; 5e) H. Sun, Q. Zhang, J. Li, S. Peng, X. Wang, R. Cai, *Nano Today* **2021**, *37*, 101073.

6) M. Bouché, C. Hognon, S. Grandemange, A. Monari, P.C. Gros, *Dalton Trans.* **2020**, *49* (33), 11451.
7) P.S. Yarmolenko, E.J. Moon, C. Landon, A. Manzoor, D.W. Hochman, B.L. Viglianti, M.W. Dewhirst, *Int. J. Hyperthermia*, **2011**, *27*, 320.
8) S. Okuyama, T. Nagaya, F. Ogata, Y. Maruoka, K. Sato, Y. Nakamura, P.L. Choyke, H. Kobayashi, *Oncotarget* **2017**, *8* (68), 113194.
9a) M. Fu, Y. Yang, Z. Zhang, Y. He, Y. Wang, C. Liu, X. Xu, J. Lin, F. Yan, *Small* **2023**, *19* (14), 2205343; b) Z. Liu, J. Wen, G. Zhou, J. Xu, L. Zhu, M. Zhang, F. Liu, Y. Zhang, *Adv. Therapeutics* **2022**, *5* (11), 2200168; c) H. Gu, W. Liu, W. Sun, J. Du, J. Fan, X. Peng, *Chem. Sci.* **2022**, *13* (33), 9719.
10a) W. Yim, J. Zhou, Y. Mantri, M.N. Creyer, C.A. Moore, J.V. Jokerst, *ACS Appl. Mater. Interfaces* **2021**, *13* (13), 14974; b) M. Bouché, M. Pühringer, A. Iturmendi, A. Amirshaghaghi, A. Tsourkas, I. Teasdale, D.P. Cormode, *ACS Appl. Mater. Interfaces* **2019**, *11* (32), 28648; c) M. Bouché, J.C. Hsu, Y.C. Dong, J. Kim, K. Taing, D.P. Cormode, *Bioconjugate Chem.* **2020**, *31* (2), 303; d) Y. Liu, L. Teng, B. Yin, H. Meng, X. Yin, S. Huan, G. Song, X.-B. Zhang, *Chem. Rev.* **2022**, *122* (6), 6850; e) J.P. Thawani, A. Amirshaghaghi, L. Yan, J.M. Stein, J. Liu, A. Tsourkas, *Small* **2017**, *13* (37), 1701300.
11a) O.S. Wenger, *Chem. Eur. J.* **2019**, *25* (24), 6043; b) D.C. Ashley, E. Jakubikova, *Coord. Chem. Rev.* **2017**, *337*, 97; c) A.R. Marri, E. Marchini, V. Diez Cabanes, R. Argazzi, M. Pastore, S. Caramori, C.A. Bignozzi, P.C. Gros, *Chem. Eur. J.* **2021**, *27* (65), 16260; d) A.R. Marri, B. Marekha, T. Penfold, S. Haacke, P.C. Gros, *Inorg. Chem. Front.* **2022**, *10* (1), 118; e) M. Huber-Gedert, M. Nowakowski, A. Kertmen, L. Burkhardt, N. Lindner, R. Schoch, R. Herbst-Irmer, A. Neuba, L. Schmitz, T.-K. Choi, J. Kubicki, W. Gawelda, M. Bauer, *Chem. Eur. J.* **2021**, *27* (38), 9905.
12a) P. Xiang, Y. Shen, Z. Feng, M. Sun, Q. Zhang, S. Li, D. Li, G. Zhang, Z. Wu, Y. Tian, Z. Zhang, X. Tian, *Inorg. Chem. Front.* **2020**, *7*, 2753; b) L. Zhang, S. Ma, T. Wang, S. Li, L. Wang, D. Li, Y. Tian, Q. Zhang, *Anal. Chem.* **2023**, *95* (2), 1635.
13) A. Jouaiti, *Synth. Commun.* **2021**, *51*, 1547.
14a) J.E. Beves, E.L. Dunphy, E.C. Constable, C.E. Housecroft, C.J. Kepert, M. Neuburger, D.J. Price, S. Schaffner, *Dalton Trans.* **2008**, *3*, 386, b) J. Nel, D. Siniscalco, C. Hognon, M. Bouché, N. Touche, E. Brunner, P.C. Gros, A. Monari, S. Grandemange, G. Francius, *Nanoscale* **2022**, *14* (7), 2735.
15) J.E. Beves, E.C. Constable, C.E. Housecroft, C.J. Kepert, M. Neuburger, D.J. Price, S. Schaffner, *Cryst. Eng. Comm.* **2007**, *9* (11), 1073.
16a) E.C. Constable, C.E. Housecroft, M. Neudburger, D. Phillips, P.R. Raithby, E. Sparr, D.A. Tocher, M. Zehnder, Y. Zimmermann, *Dalton Trans.* **2000**, 2219; b) E.C. Constable, E.L. Dunphy, C.E. Housecroft, W. Kylberg, M. Neuburger, S. Schaffner, E.R. Schofield, C.B. Smith, *Chem. Eur. J.* **2006**, *12*, 4600; c) A. Winter, U.S. Schubert, *Macromol. Chem. Phys.* **2007**, *208* (18), 1956.
17a) M.N. Hopkinson, C. Richter, M. Schedler, F. Glorius, *Nature* **2014**, *510* (7506), 485; b) A. Gautier, F. Cisnetti, *Metallomics* **2012**, *4* (1), 23.
18) C. Förster, M. Dorn, T. Reuter, S. Otto, G. Davarci, T. Reich, L. Carrella, E. Rentschler, K. Heinze, *Inorganics* **2018**, *6* (3), 86.
19) T. Duchanois, T. Etienne, M. Beley, X. Assfeld, E.A. Perpète, A. Monari, P.C. Gros, *Eur. J. Inorg. Chem.* **2014**, *2014* (23), 3747.
20) M.L. Landry, J.J. Crawford, *ACS Med. Chem. Lett.* **2020**, *11* (1), 72.

21) M. Bouché, A. Bonnefont, T. Achard, S. Bellemin-Laponnaz, *Dalton Trans.* **2018**, *47* (33), 11491.
22) C.P. Satori, V. Kostal, E.A. Arriaga, *Anal. Chem.* **2011**, *83* (19), 7331.
23) S. Keller, Y.C. Ong, Y. Lin, K. Cariou, G. Gasser, *J. Organomet. Chem.* **2020**, *906*, 121059.
24) G. Kalot, A. Godard, B. Busser, M. Bendellaa, F. Dalonneau, C. Paul, X.L. Guével, V. Josserand, J.-L. Coll, F. Denat, E. Bodio, C. Goze, T. Gautier, L. Sancey, *Biomater. Sci.* **2022**, *10* (21), 6315.
25a) H.J. Vreman, R.J. Wong, D.K. Stevenson, R.K. Route, S.D. Reader, M.M. Fejer, R. Gale, D.S. Seidman, *Pediatr. Res.* **1998**, *44* (5), 804; b) M. Piksa, C. Lian, I.C. Samuel, K.J. Pawlik, I.D.W. Samuel, K. Matczyszyn, *Chem. Soc. Rev.* **2023**, *52*, 1697.
26) E.M. Kercher, K. Zhang, M. Waguespack, R.T. Lang, A. Olmos, B.Q. Spring, *J. Biomed. Optics* **2020**, *25* (6), 063811.
27) X. Li, J.F. Lovell, J. Yoon, X. Chen, *Nat. Rev. Clin. Oncol.* **2020**, *17*, 657.
28a) S. Paul, P. Kundu, P. Kondaiah, A.R. Chakravarty, *Inorg. Chem.* **2021**, *60* (21), 16178; b) U. Basu, I. Khan, A. Hussain, B. Gole, P. Kondaiah, A.K. Chakravarty, *Inorg. Chem.* **2014**, *53* (4), 2152; c) U. Basu, M. Roy, A.R. Chakravarty, *Coord. Chem. Rev.* **2020**, *417*, 213339; d) L. Gourdon, K. Cariou, G. Gasser, *Chem. Soc. Rev.* **2022**, *51* (3), 1167.
29a) C.S. Jackson, S. Schmitt, Q.P. Dou, J.J. Kodanko, *Inorg. Chem.* **2011**, *50* (12), 5336; b) X. Jiang, L. Chen, X. Wang, L. Long, Z. Xiao, X. Liu, *Chem. Eur. J.* **2015**, *21* (37), 13065.
30) D.C. Ashley, E. Jakubikova, *Inorg. Chem.* **2018**, *57* (16), 9907.
31a) J.D. Braun, I.B. Lozada, C. Kolodziej, C. Burda, K.M.E. Newman, J. van Lierop, R.L. Davis, D.E. Herbert, *Nat. Chem.* **2019**, *11* (12), 1144; b) J.D. Braun, I.B. Lozada, D.E. Herbert, *Inorg. Chem.* **2020**, *59* (23), 17746; c) P. Dierks, A. Päpcke, O.S. Bokareva, B. Altenburger, T. Reuter, K. Heinze, O. Kühn, S. Lochbrunner, M. Bauer, *Inorg. Chem.* **2020**, *59* (20), 14746; d) S. Mukherjee, D.E. Torres, E. Jakubikova, *Chem. Sci.* **2017**, *8* (12), 8115.
32) T. Ohmura, Y. Morimasa, M. Suginome, *J. Am. Chem. Soc.* **2015**, *137* (8), 2852.

Experimental section

Manipulations of air and moisture sensitive compounds were carried under argon atmosphere using standard Schlenk techniques and freshly distilled solvents. Reagents were purchased from chemical suppliers (Sigma Aldrich Europe, BLDpharm Europe) and used without further purification. ^{1}H and ^{13}C Nuclear Magnetic Resonance (NMR) spectra were recorded on a Bruker Avance III 400 spectrometer at 295 K, using residual solvent peak as a reference. LC-MS investigations were performed on a MicroToFq Bruker coupled to a LC U3000 Thermo. IR spectra were acquired on a Shimadzu IRAffinity-1. Cyclic voltammetry was performed on a Radiometer PST006 potentiostat using a conventional three-electrode cell. Absorbance spectra were recorded on a Lambda 1050 Perkin Elmer (Shelton CT), and fluorescence spectra on a Horiba-Jobin Yvon Fluorolog 3 (Edison NJ), at 20°C. Photoacoustic images were acquired on a TRITOM PhotoSound (Houston TX) at 36°C, using a nanosecond pulsed laser EKSPLA PhotoSonus ranging from 330-1320 nm (Vilnius, Lituania). Photothermal therapy experiments were carried out using a custom setup using elements from ThorLabs (Germany): LEDs (565 nm 1000 mA, 660 nm 1200 mA, 730 nm 1000 mA) collimated with an adjustable collimation adapter

SM2F32, power was measured with a thermal sensor power meter PM160T and temperature was recorded using a thermal camera optris Xi 400 « spot finder » (Optris, Germany).

General procedure for the synthesis of [Fe(tpy-Me)$_2$]4I complexes

Iodomethane (306 µmol) is dropped under argon to a solution of [Fe(tpy)$_2$]2Cl (15µmol) in dried DMF (5 mL) in a sealed flask. The mixture is heated at 130°C for 1h, allowed to cooldown and supplemented with 1 mL MeOH prior further precipitated by addition to 20 mL Et_2O. The fine powder is recovered by centrifugation (6 krpm, 5 min). Upon purification on reversed phase semi-preparative HPLC using a H_2O-MeOH gradient, the desired complex is obtained as dark purple-blue solid.

4a. [Fe(1''-methyl-6'-(pyridin-2-yl)-[2,2':4',4''-terpyridin]-1''-ium)2]4I

Purple powder (37%). ^{1}H NMR (d$_6$-DMSO, 400 MHz, 25°C): δ 4.48 (s, 6H, CH3), 7.17 (m, 4H, CHar), 7.25 (m, 4H, CHar), 7.99 (m, 4H, CHar), 8.85 (m, 4H, CHar), 9.00 (m, 4H, CHar), 9.64 (s, 4H, CHar); ^{13}C NMR (d$_6$-DMSO, 101 MHz, 25°C): δ 48.8, 122.7, 125.3, 126.6, 128.8, 140.1, 143.5, 146.9, 152.1, 153.5, 157.9, 161.1; HRMS (ESI) calcd for $C_{42}H_{34}FeN_8$ m/z=176.5558, found 176.5572 [M^{2+}].

4b. [Fe(1''-methyl-6'-(pyridin-3-yl)-[2,2':4',4''-terpyridin]-1''-ium)2]4I

Purple powder (81%). ^{1}H NMR (d$_6$-DMSO, 400 MHz, 25°C): δ 4.67 (s, 6H, CH3), 7.24 (m, 4H, CHar), 7.30 (d, J=5.4 Hz, 4H, CHar), 8.12 (dt, 4H, J=7.7 Hz and 1.3 Hz, CHar), 8.63 (m, 2H, CHar), 9.00 (d, J=8.1 Hz, 4H, CHar), 9.34 (d, J=6.1 Hz, 2H, CHar), 9.65 (d, J=8.1 Hz, 2H, CHar), 9.89 (s, 4H, CHar), 10.19 (s, 2H, CHar); ^{13}C NMR (d$_6$-DMSO, 101 MHz, 25°C): δ 48.7, 121.5, 124.3, 127.9, 128.2, 135.7, 139.2, 142.1, 142.9, 144.7, 146.6, 152.8, 157.3, 160.3; HRMS (ESI) calcd for $C_{42}H_{34}FeN_8$ m/z=176.5558, found 176.5572 [M^{2+}].

4c. [Fe(1''-methyl-6'-(pyridin-4-yl)-[2,2':4',4''-terpyridin]-1''-ium)2]4I

Dark blue powder (94%). ^{1}H NMR (d$_6$-DMSO, 400 MHz, 25°C): δ 4.80 (s, 6H, CH3), 7.29 (m, 4H, CHar), 7.46 (d, J=5.5 Hz, 4H, CHar), 8.09 (m, 4H, CHar, 8.52 (t, J=7.1 and 1.4 Hz, 2H, CHar), 8.76 (d, J=7.9 Hz, 2H, CHar), 8.81 (d, J=7.9 Hz, 2H, CHar), 9.06 (t, J= 7.9Hz, 2H, CHar), 9.50 (d, J=6.2 Hz, 2H, CHar), 9.66 (s, 4H, CHar); ^{13}C NMR (d$_6$-DMSO, 101 MHz, 25°C): δ 48.8, 122.7, 125.3, 126.5, 128.7, 140.0, 143.5, 146.9, 152.0, 153.4, 157.8, 161.1; HRMS (ESI) calcd for $C_{42}H_{34}FeN_8$ m/z=176.5558, found 176.5577 [M^{2+}].

6. [Fe(4-pyridyl-(2,6-bis(3-methyl-imidazol)pyridine)2]2PF6

To a solution of imidazolium salt **5** (0.077 g, 0.126 mmol) in 2 mL of anhydrous DMF was added $FeCl_2$ (0.008 g, 0.063 mmol) and degassed the mixture with Argon for 10 min. Then added t-BuOK (0.071 g, 0.632 mmol) to the above mixture and stirred at room temperature for 20 min. A saturated solution of NH_4PF_6 was added (10 ml) and the precipitate was collected by filtration. Then the crude was further purified on silica gel column chromatography using acetone/H_2O/KNO_3(sat) = 10: 3: 0.5 mixture. The pinkish fraction was collected and after the evaporation of acetone, the left solution was treated with a saturated solution of NH_4PF_6. Affording the precipitation of the desired complex, it was then filtered, washed with distilled water followed by ether, and dried under vacuum. The isolated complex **6** was obtained as a red powder (0.035 g, 56% yield). ^{1}H NMR (400 MHz, DMSO-d$_6$, δ ppm): 9.03(d, J= 5.74 Hz, 2H), 8.77(s, 2H), 8.64(s, 2H), 8.36(d, J= 5.42 Hz, 2H), 7.41(s, 2H), 2.58(s, 6H). HRMS (ESI) calcd for $C_{36}H_{32}FeN_{12}$ m/z = 344.1106. Found: 344.1134 [M-2PF6]. Of note, the too low solubility of this complex in DMSO prevented the acquisition of ^{13}C NMR.

7. [Fe(4-pyridynium-(2,6-bis(3-methyl-imidazol)pyridine)2]4PF6

Complex **6** (0.015 g, 0.015 mmol) was charged in a 10 mL round bottomed flask and dissolved in 1 mL of DMF. Then added methyl iodide (0.010 mL, 0.153 mmol) and stirred at RT for 24 h. Desired complex was precipitated upon addition of saturated NH_4PF_6 solution and stirred until the product is completely precipitated. Complex **7** was collected by vacuum filtration and washed 3 times with water and then diethyl ether and dried under vacuum. The isolated complex **7** was obtained as dark blue powder (0.017 g, 85% yield). ^{1}H NMR (400 MHz, CD_3CN, δ ppm): 8.89(d, J= 6.77 Hz, 2H), 8.59(d, J= 6.96 Hz, 2H), 8.25(s, 2H), 8.18(d, J= 2.20 Hz, 2H), 7.10(d, J= 2.20 Hz, 2H), 4.44(s, 3H), 2.60(s, 6H). ^{13}C NMR (100 MHz, CD_3CN, δ ppm): 199.28, 155.11, 152.70, 146.73, 143.20, 127.80, 126.26, 117.25, 104.25, 48.80, 35.36. HRMS (ESI) calcd for C38H36FeN12 m/z = 358.1262. Found: 358.1262 [M-2PF6], $C_{38}H_{37}FeN_{12}$ m/z = 239.0866. Found: 239.0878 [M-3PF6].

Table of contents:

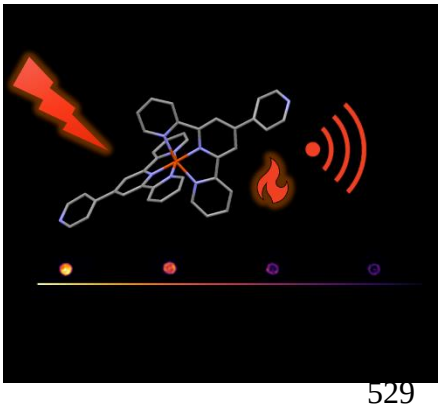

Iron(II) complexes bearing terpyridine or 4-pyridin-2,6-bis N-heterocyclic carbene-pyridine ligands display light-triggered photoactivation for theranostic application. Their irradiation promotes a non-radiative decay that can be exploited in photoacoustic imaging or photothermal therapy.

Biography:

Mathilde Bouché received her PhD in Bioinorganic Chemistry from the University of Strasbourg (France) in 2017 under the supervision of Dr. S. Bellemin-Laponnaz. After two postdoctoral stays as Fulbright scholar at Prof. Cormode's lab at the University of Pennsylvania (U.S.), and at the University of Lorraine (France), she started her independent career in 2020 as a CNRS research Associate Professor at the University of Lorraine (France). Her interdisciplinary research focusses on metal-based complexes for therapeutic and theranostic applications.